

Direct Measurement of Water Cluster Concentrations by Infrared Cavity Ringdown Laser Absorption Spectroscopy

J. B. Paul,* C. P. Collier, and R. J. Saykally

Department of Chemistry, University of California at Berkeley, Berkeley, California 94720

J. J. Scherer and A. O'Keefe

Los Gatos Research, 1685 Plymouth, Mountain View, California 94043

Received: April 8, 1997[⊗]

The recently developed technique of infrared cavity ringdown laser absorption spectroscopy (IR-CRLAS) has been employed in the 3.0 μm region to determine the absolute concentrations of water dimers, trimers, tetramers, and pentamers in a pulsed supersonic expansion for the first time. Additional spectral features are reported, one of which we assign to the bound O–H stretching bands of the hexamer. Additionally, by simple variation of the jet stagnation pressure, the collective O–H stretching absorption from all clusters produced in the expansion was observed to change from that of discrete features of small clusters to band profiles of liquid water and finally to amorphous ice.

Water clusters have recently been implicated in the important atmospheric processes of acid rain formation^{1,2} and the anomalous absorption of radiation in clouds,^{3,4} although the detailed mechanisms are not well understood. To advance our knowledge of these phenomena, it would be highly advantageous to have a sensitive *in situ*, nonintrusive probe of the concentrations of the individual water clusters. In this Letter we report the application of a simple and powerful ultrasensitive absorption method for measuring infrared spectra, infrared cavity ringdown laser absorption spectroscopy (IR-CRLAS), which can achieve this end. We demonstrate this technique in the 3 μm spectral region by determining the absolute concentrations of small water clusters ($(\text{H}_2\text{O})_n$, $n = 2-5$) formed in a pulsed slit-jet supersonic expansion.⁵

Prior to the vibration–rotation–tunneling (VRT) spectroscopy experiments now being carried out in the terahertz (far-infrared) region of the spectrum,⁶ water clusters have been studied primarily in the mid-IR region, either by matrix isolation absorption spectroscopy,^{7,8} or by some type of “action” spectroscopy in molecular beams, wherein the absorption of IR photons is monitored via a dynamically coupled event (dissociation,^{9,10} ionization,¹¹ bolometric response^{12,13}). Absorption intensity information (e.g. concentrations) can be extracted from matrix isolation studies, although perturbations to the spectrum by the environment are often severe. With action methods, isolated individual clusters can be probed because of the extremely high sensitivity attainable, but concentration information is often lost because of the unclear coupling between the photon absorption and the resulting dynamics.

CRLAS combines the advantages of the above methods by providing the ability to probe gaseous samples with both extremely high sensitivity and with quantitative and reproducible absorption intensity information. The high sensitivity is derived from measuring the *rate* (rather than magnitude) of absorption of a light pulse by a sample placed within a closed optical cavity.¹⁴ Provided the absorption occurs linearly for a single pass of the pulse through the sample, the intensity of the pulse within the cavity decays exponentially in time due to the constant fractional round-trip losses of the system. This decay

time is the experimentally measured quantity and essentially comprises up to tens of thousands of round-trip absorption events occurring over a microsecond time scale. Dividing the absorption rate by the cavity optical round-trip frequency yields the per pass sample absorbance after the per-pass intensity loss from the empty cavity is subtracted. Therefore, given knowledge of the absorption cross section and the per pass absorption path length, the absolute concentration of the absorbing species can be determined directly.

Scherer et al.¹⁵ recently described the initial extension of cavity ringdown laser absorption spectroscopy (CRLAS) into the infrared (IR) region using a high-resolution (0.005 cm^{-1}) laser, following our applications in the UV–visible for studies of laser-generated metal-containing species in pulsed supersonic jets.¹⁶ Here we employ a low-resolution (0.2 cm^{-1}) version of the experiment based on Raman shifting the output of a pulsed dye laser, which allows the broad range of O–H stretch frequencies ($3000-3800\text{ cm}^{-1}$) to be scanned quickly and easily. The CRLAS method offers at least 2 orders of magnitude greater sensitivity than state-of-the-art FTIR techniques and possesses a compelling degree of simplicity. As it does not require large amounts of laser power ($100\text{ }\mu\text{J/pulse}$ is sufficient for use with a standard InSb infrared detector and 99.99% reflective cavity mirrors) or a well-defined molecular beam (as do “indirect” techniques previously used to study water clusters^{9,10,12,13,17}), construction of a very compact system can be envisioned. Such a new spectrometer would markedly enhance the prospects for measuring water clusters in atmospheric monitoring experiments. Details of the CRLAS experiment are summarized in Figure 1.

Figure 2 shows IR-CRLAS spectra obtained for three relatively low cluster source pressures. The assignments shown here for clusters as large as $(\text{H}_2\text{O})_5$ are taken from the recent work of Huisken et al.,¹⁷ who employed a mass selective vibrational predissociation technique. The broad background feature upon which these bands are superimposed is attributable to clusters larger than pentamer.¹⁸ To obtain accurate integrated absorbance values for the smaller cluster bands, this background must be removed by assuming that it contributes smoothly to the spectrum and subtracting it.

Our ability to extract accurate water cluster number densities from integrating absorption bands present in the resulting

[⊗] Abstract published in *Advance ACS Abstracts*, June 15, 1997.

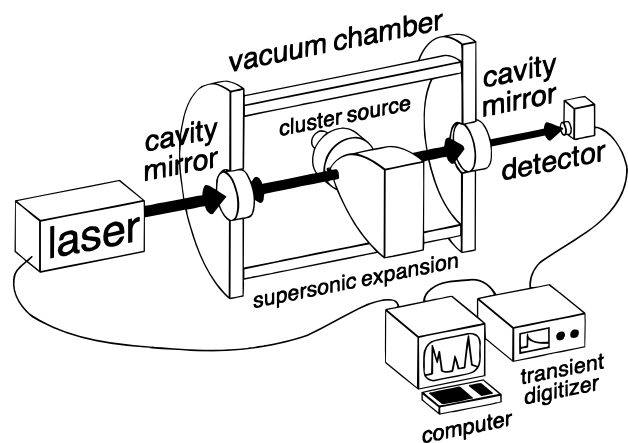


Figure 1. IR-CRLAS apparatus. Tunable infrared radiation is generated by directing the output of a pulsed dye laser into a multipass hydrogen Raman shifter. After filtering, the $3\ \mu\text{m}$ output (3rd Stokes) is coupled into the ringdown cavity. The cavity mirrors press against o-rings to seal the Roots-pumped vacuum chamber against atmosphere. Inside the chamber, the ringdown pulse intersects a pulsed slit jet expansion in which the water clusters are formed. The water is seeded into the expansion by bubbling helium carrier gas through the room temperature liquid. The light transmitting the output mirror is focused into an InSb detector. The resulting signal is amplified, digitized, and sent to a PC where it is fit to a first-order exponential, which is directly related to the total cavity loss per laser pass. The PC additionally controls the scanning of the dye laser. Base line losses are determined by scanning the laser with the expansion turned off and are then subtracted from the data, yielding the absolute sample absorbance, from which the carrier concentrations are extracted.

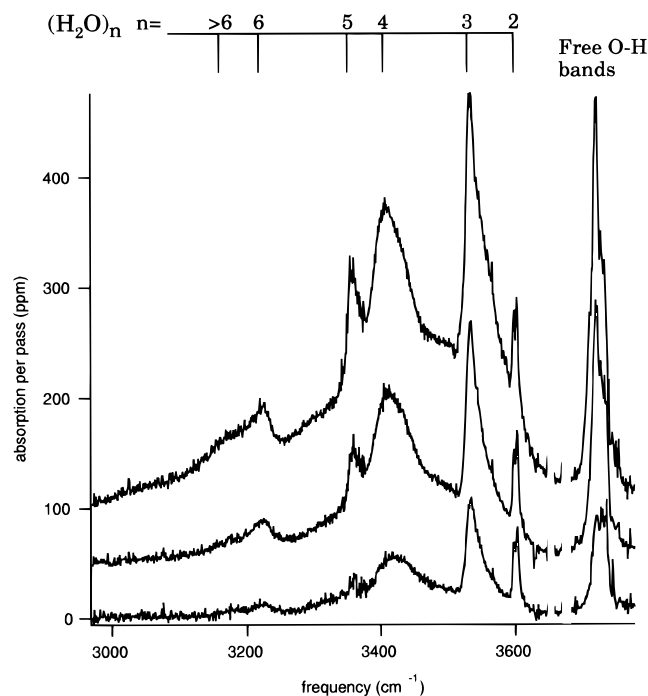


Figure 2. IR-CRLAS data obtained for source backing pressures of (from bottom to top) 10, 12.5, and 15 psi absolute pressure. The assignments for clusters up to $(\text{H}_2\text{O})_5$ are adopted from ref 10.

spectrum is potentially limited by several factors, which are addressed here: (1) Accurate integrated absorbance values are only obtained when the conditions of Beer's Law are satisfied. These conditions should hold in the present case, as present and previous work with high-resolution lasers ($\Delta\nu = 1\ \text{MHz}$) reveal only diffuse structure in the dimer band at $3600\ \text{cm}^{-1}$ and a virtual continuum absorption by the trimer peaking at $3532\ \text{cm}^{-1}$.¹³ (2) Bands due to different carriers may not be

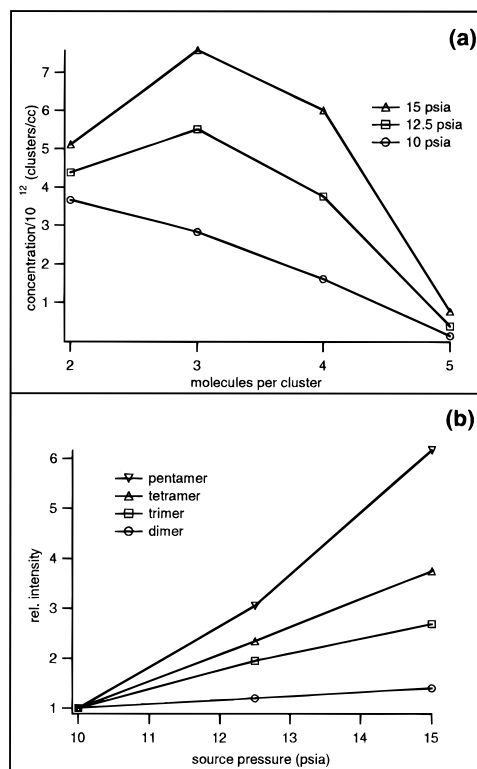


Figure 3. (a) Plot of water cluster absolute concentration in the expansion vs cluster size for the three source pressures shown in Figure 2. (b) Plot of relative peak band intensity vs source pressure. Information about the relative carrier size is obtained through this analysis.

completely resolved from one another. Previous work indicates that a single carrier can be assigned to each individual band.^{17,19} The present results support this through the observation that the band shapes do not change appreciably as the bands themselves grow in intensity. (3) The integrated band strengths of these clusters have not been determined experimentally, necessitating the use of *ab initio* estimates.²⁰ To the best of our knowledge, the most accurate complete set of estimates for these intensities for the range of clusters measured here are computed at the SCF level and are expected to be only approximate, as calculations at this level of theory almost always overestimate the IR band intensity. This introduces the most significant uncertainty in the determined water cluster number densities, which therefore are best regarded as lower bounds. Both of these latter two uncertainties will undoubtedly be considerably reduced as more sophisticated *ab initio* calculations of band intensities become available for small water clusters.

The water cluster densities measured in the pulsed supersonic expansion are plotted in Figure 3a. Perhaps the most striking observation is that the water trimer is apparently the most abundant cluster in the expansion, even at fairly low source pressure. Supporting this result is the fact that when compared with the larger clusters the per monomer binding energy of the trimer is discontinuously larger than that of the dimer.²¹ This extra stabilizing energy results from the extra hydrogen bond effected by the ring structure of the trimer (three total), compared with the single bond in the dimer. On the other hand, there exists the distinct possibility that double-donor modes of the cage structures of the $n > 6$ clusters are contributing to the absorption in this region.¹¹ However, this component should be small at the lower source pressures. Furthermore, the sharpness of lower frequency edge of the trimer band provides a very good gauge of the relative concentration. From this, it

is quite clear that the trimer abundance is increasing rapidly over this pressure range.

Overall, the determined cluster concentrations appear quite reasonable; we find lower bounds of 5×10^{12} dimers, 7×10^{12} trimers, 5×10^{12} tetramers, and 1×10^{12} pentamers for a source pressure of 1 atm. These figures do not account for the overestimation of the IR intensities by the ab initio calculations, which, as mentioned earlier, are most likely ca. 50% too large. We should point out that only a small region of the expansion approximately 2–3 mm from the orifice was probed in the present study and that the distribution of clusters certainly changes with spatial position.

As expected, the peak in the distribution of cluster sizes shifts slightly toward larger clusters with increasing source pressure. This change is more easily discerned by plotting the relative peak intensities as a function of pressure (Figure 3b). The slopes of these lines are steepest for the pentamer, while nearly flat for the dimer, which is consistent with the well-known assumption that higher source backing pressure favors the formation of larger clusters. Interpreting the results in this manner provides additional confirmation of the carrier identities of the individual bands, which is generally difficult to obtain in direct absorption experiments when rotational resolution is not achieved.

Other features appearing in the spectrum over a similar pressure range as does the water pentamer absorption are two partially resolved bands at 3220 and 3170 cm^{-1} , with the former band clearly growing in prior to the latter with increasing pressure. We assign the 3220 cm^{-1} absorption to $(\text{H}_2\text{O})_6$ and allow for the possibility of additional absorption in this region from $(\text{H}_2\text{O})_7$. From the observed pressure dependence, the 3170 cm^{-1} band most likely belongs to clusters larger than those responsible for the 3220 cm^{-1} feature. Therefore, we tentatively assign this band to $(\text{H}_2\text{O})_8$. The following evidence strongly supports these conclusions. Ab initio studies of $(\text{H}_2\text{O})_8$ indicate that bands occurring in this region as well as the 3600 cm^{-1} region could serve as chromophores signifying the presence of cage-like structures containing both double hydrogen bond donors ($\sim 3600 \text{ cm}^{-1}$) and single donors ($\sim 3200 \text{ cm}^{-1}$).²⁰ Pribble and Zwier¹¹ have used these results to rationalize their spectra of benzene–water clusters, which show bands in the 3500 and 3200 cm^{-1} regions for clusters containing six or more water monomers, which apparently proves a noncyclic water cluster configuration within the benzene–water complex. Additionally, $(\text{H}_2\text{O})_6$ has recently been determined to be the first noncyclic pure water cluster and is found to be produced abundantly in these types of expansions.²² Furthermore, the spectra of water clusters in argon matrices show a feature at 3200 cm^{-1} which appears at higher deposition concentrations than does the pentamer band (at 3320 cm^{-1} in the matrix).^{7,8} Interestingly, many years ago Coker et al.¹² reported weak bands at these exact locations, which they tentatively assigned to the donor and acceptor bend overtones of the dimer. If these are the same bands observed here, their assignments must be incorrect, as the pressure dependence of these bands is far more similar to the pentamer than to the dimer. Concerning the associated double-donor bands expected to lie near 3550 cm^{-1} , there does appear to be some absorption in this region underlying the trimer band, but due to this interference, no conclusive information can be reported at this time.

Figure 4 shows the results of increasing the pressure beyond the range considered above (> 15 psi). For reference, the 15 psi scan shown in Figure 2 is included in the lowest region of the figure, while the remaining scans were taken at 10 psi increments, beginning with 25 psi. Distinct changes in the spectrum occur over this range of pressures, primarily in the

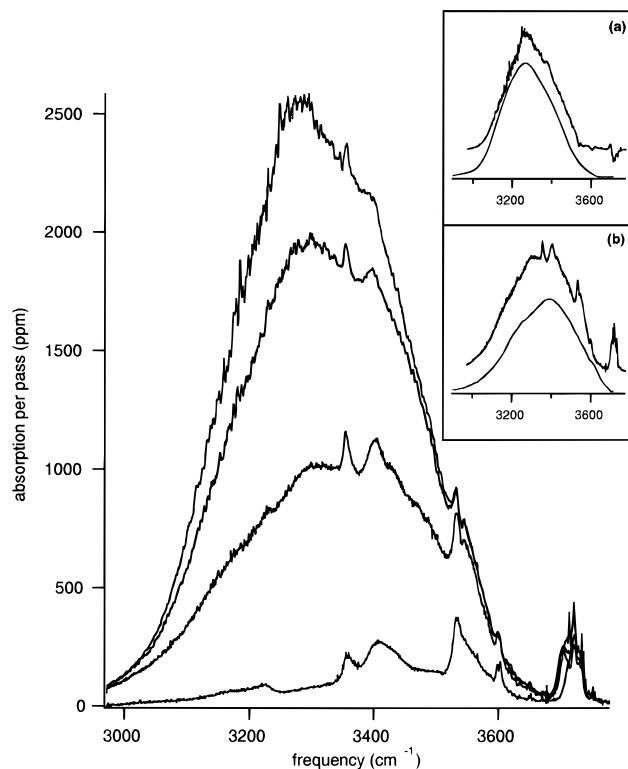


Figure 4. IR-CRLAS spectra obtained for source backing pressures of 15, 25, 35, and 45 psi (bottom to top). Inset a: The difference between the 45 psi spectrum and the 25 psi spectrum (upper curve) shows a strong resemblance to the spectrum of bulk amorphous ice (data taken from ref 23). Inset b: The 25 psi IR-CRLAS spectrum (upper curve) is compared with the spectrum of liquid water (data taken from ref 25). In both insets, the IR-CRLAS data is displaced vertically for clarity.

occurrence of a broad continuum that grows dramatically and shifts to lower frequency with increasing pressure. Superimposed on this much larger, broad feature are the discrete bands due to the smaller clusters. Progressively larger clusters are undoubtedly responsible for the changes to the spectrum over this range of pressures. In fact, by subtracting the 25 psi data from the 45 psi data, we can effectively remove the portion of the spectrum due to small and “intermediate” sized clusters to show (Figure 4 inset, upper) that a population of clusters large enough to quite accurately reproduce the spectrum of bulk amorphous ice²³ account for these new spectral features. Interestingly, even at the highest backing pressure in this study, the dimer band at 3600 cm^{-1} is still clearly observable, indicating that, for these pressure ranges, clusters ranging in size from the dimer to what may be considered bulk coexist in the expansion.

By integrating this band and using the per monomer absorption cross section of amorphous ice,²³ we estimate the total number of water molecules present in the form of these very large clusters to be $\sim 10^{15}$ molecules/ cm^3 . Assuming an average cluster size 10^4 molecules/cluster,²⁴ we obtain a rough estimate of 10^{11} “ice nanoparticles”/ cm^3 . This is generally consistent with the $\sim 10^{13}$ clusters/ cm^3 quantity derived for the smaller clusters.

Finally, we can compare our IR-CRLAS spectra with that of liquid water in the O–H stretching region, which exhibits a broader, blue-shifted absorption spectrum compared with virtually all forms of ice.²⁵ Over the range of pressures studied in the present work, the best match is clearly with the spectrum obtained at 25 psi (Figure 4 inset, lower). In this case, we have a distribution of “intermediate” sized clusters contributing to

the spectrum, the majority of which most likely contain less than a few hundred water molecules per cluster. The structures of these clusters are thought to be very similar to what would be obtained if liquid water was "instantaneously" frozen.²⁴ Therefore, by virtue of the distribution of cluster sizes, to some degree both the finite interaction length in the liquid and the inherent randomness of this interaction are approximated.

Acknowledgment. This work was supported by the Air Force Office of Scientific Research (Grant F49620-96-1-0411) and the National Science Foundation (Grant CHE-9424482).

References and Notes

- (1) Kolb, C. E.; Jayne, J. T.; Worsnop, D. R.; Molina, M. J.; Meads, R. F.; Viggiano, A. A. *J. Am. Chem. Soc.* **1994**, *116*, 10314.
- (2) Morokuma, K.; Muguruma, C. *J. Am. Chem. Soc.* **1994**, *116*, 10316.
- (3) Li, Z.; Barker, H. W.; Moreau, L. *Nature* **1995**, *376*, 486.
- (4) Cess, R. D.; Zhang, M. H.; Minnis, P.; Corsetti, L.; Dutton, E. G.; Forgan, B. W.; Garber, D. P.; Gates, e. a. W. L. *Science* **1995**, *267*, 496.
- (5) Liu, K.; Fellers, R. S.; Viant, M. R.; McLaughlin, R. P.; Brown, M. G.; Saykally, R. J. *Rev. Sci. Instrum.* **1996**, *67*, 410.
- (6) Liu, K.; Cruzan, J. D.; Saykally, R. J. *Science* **1996**, *271*, 929.
- (7) Ayers, G. P.; Pullin, A. D. E. *Spectrochim. Acta* **1976**, *32A*, 1629.
- (8) Brentwood, R. M.; Barnes, A. J.; Orville-Thomas, W. J. *J. Mol. Spectrosc.* **1980**, *84*, 391.
- (9) Vernon, M. F.; Krajnovich, D. J.; Kwok, H. S.; Lisy, J. M.; Shen, Y. R.; Lee, Y. T. *J. Chem. Phys.* **1982**, *77*, 47.
- (10) Page, R. H.; Frey, J. G.; Shen, Y. R.; Lee, Y. T. *Chem. Phys. Lett.* **1984**, *106*, 373.
- (11) Pribble, R. N.; Zwier, T. S. *Science* **1994**, *265*, 75.
- (12) Coker, D. F.; Miller, R. E.; Watts, R. O. *J. Chem. Phys.* **1985**, *82*, 3554.
- (13) Huang, Z. S.; Miller, R. E. *J. Chem. Phys.* **1989**, *91*, 6613.
- (14) Scherer, J. J.; Paul, J. B.; O'Keefe, A.; Saykally, R. J. *Chem. Rev.* **1997**, *97*, 25.
- (15) Scherer, J. J.; Voelkel, D.; Rakestraw, D. J.; Paul, J. B.; Collier, C. P.; Saykally, R. J.; O'Keefe, A. *Chem. Phys. Lett.* **1995**, *245*, 273.
- (16) Paul, J. B.; Scherer, J. J.; Collier, C. P.; Saykally, R. J. *J. Chem. Phys.* **1996**, *104*, 2782.
- (17) Huisken, F.; Kaloudis, M.; Kulcke, A. *J. Chem. Phys.* **1996**, *104*, 17.
- (18) Paul, J. B.; Provencal, R.; Collier, C. P.; Saykally, R. J., in preparation.
- (19) Fröchtenicht, R.; Kaloudis, M.; Koch, M.; Huisken, F. *J. Chem. Phys.* **1996**, *105*, 6128.
- (20) Knochenmuss, R.; Leutwyler, S. *J. Chem. Phys.* **1992**, *96*, 5233.
- (21) Xantheas, S. S. *J. Chem. Phys.* **1995**, *102*, 4505.
- (22) Liu, K.; Brown, M. G.; Carter, C.; Saykally, R. J.; Gregory, J. K.; Clary, D. C. *Nature* **1996**, *381*, 501.
- (23) Hagen, W.; Tielens, A. G. G. M.; Greenberg, J. M. *Chem. Phys.* **1981**, *56*, 367.
- (24) Torchet, G.; Schwartz, P.; Farges, J.; deFeraudy, M. F.; Raoult, B. *J. Chem. Phys.* **1983**, *79*, 6196.
- (25) *Raman and Infrared Spectral Investigations of Water Structure*; Walrafen, G. E. Ed.; Plenum Press: New York, 1972; Vol. 1.